Ruggedized Compact Microwave Probes for Mapping Material Properties of Structures

John W. SCHULTZ [1], James G. MALONEY [1], Kathleen CUMMINGS-MALONEY [1], Rebecca B. SCHULTZ [1], Juan G. CALZADA [2], Bryan C. FOOS [3]
[1]Compass Technology Group, Roswell, GA USA, john.schultz@compasstech.com
[2]Air Force Research Laboratory, Dayton, OH, USA, juan.calzada@us.af.mil
[3]First Principles, Inc, Dayton, OH, USA, bryan.foos.ctr@us.af.mil

Abstract
Microwave properties of dielectric and magnetic materials can be obtained non-destructively in a laboratory setting with a free-space focused beam device or an admittance tunnel lined with absorber. However, these systems are far from portable and may be impractical for use in a manufacturing environment. Instead, a portable and rugged microwave sensor is of interest for characterization of larger structures that don't easily fit within the geometry of a laboratory system. This paper describes the use of a new microwave probe design that is optimized to interrogate a small area of a material or component, and determine reflection or transmission properties in the 2 to 20+ GHz range. This probe is ruggedized for use in harsh environments and is optimized to have a standoff of 25 to 100 mm from the material under test. Additionally, this paper describes the integration of this probe with industrial robots to spatially map the dielectric properties of flat or curved structures. Example measurements are shown of a multilayer structure of dielectric constituents, where one or two-dimensional maps show spatially dependent properties.

Keywords: microwave mapping probe, dielectric permittivity, sheet impedance, delamination, free space measurement

1. Introduction

Free space methods have been a popular means for characterizing microwave properties of materials. This is because they enable the use of plane-wave approximations for analyzing measured data and for inverting intrinsic material properties such as dielectric permittivity, magnetic permeability, or sheet impedance. They also are non-contact, so even in a laboratory setting may be used for non-destructive evaluation of specimens. An increasingly popular apparatus for free-space measurement is the focused beam system [1], which incorporates focusing elements to direct energy from a feed antenna onto a material specimen. The use of focusing elements such as dielectric lenses or parabolic reflectors improves measurement accuracy by controlling the wave front to better simulate plane-wave illumination. However such an apparatus is necessarily electrically large, and may not be conducive to use in a harsh environment.

In a manufacturing or field environment, the components-under-test may be too large for mounting in a traditional laboratory free space fixture. In this case it is necessary to have a measurement sensor that is small enough to be brought to the component-under-test rather than the other way around. Thus a compact and ruggedized sensor is preferred, where measurements of material specimens are done 'in-situ.' This paper discusses just such a sensor and examines some possible measurement scenarios that are enabled by this sensor.

2. Microwave Mapping Probes

The use of spot probes for free space microwave material measurements goes back to at least the mid 1970s. Musil, Zacek, et al. used dielectric antennas to measure transmission through a material specimen and their sensors consisted of dielectric rods inserted into the ends of metal horn antennas [2]. They used their sensors to successfully determine the complex dielectric permittivity of Si specimens at millimeter wave frequencies. More recently Diaz et al. designed 'polyrod' antennas using computational simulation tools. Their sensor included multiple layers inserted into a metal horn antenna [3], and their innovation was to use computational tools to optimize the inserted polymer material and optimize impedance match of the probe antenna.

The spot probe described in this paper also includes both metallic elements and dielectric material. However while previous spot probes designed dielectric rods into conventional horn antennas, the present probe design was conceived by optimizing both the dielectric shape and metallic elements into an integrated unit. Figure 1 includes a photograph of these integrated spot probes showing their compact shape. The probes are fed with a single SMA port in the rear, and they transmit and receive with linear polarization from 2.5 to 20 GHz for the larger model and from 4 to 24 GHz for the smaller model. These probes are 18 cm (7 inches) and 10.2 cm (4 inches) in length for the larger and smaller variants respectively. Also shown in Figure 1 is the measured voltage standing wave ratio (VSWR) for two different large probes, which shows that the VSWR is better than 3 for the entire frequency band of use, and is better than 2 for most of that same band. The smaller probes have similar VSWR characteristics, except that they work to higher frequencies.

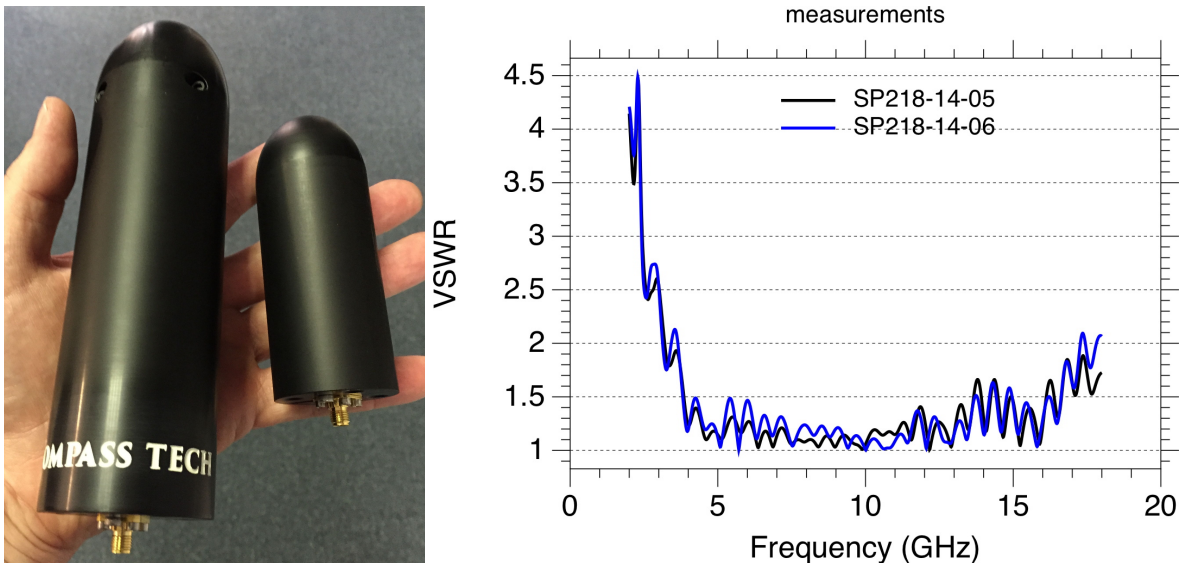

Figure 1. Photograph of large and small spot probes (left), and typical VSWR measured for the large probes (right).

Other characteristics of these probes have been presented elsewhere [9], and they have been shown to have measurement accuracies similar to laboratory focused beam systems when measuring materials at normal incidence. The illumination area is approximately round and has a diameter that depends on standoff distance as well as on frequency. For the measurements discussed in this paper, a standoff distance of approximately 7 cm (2.75") was

used and the illumination area diameter is approximately 5 cm at 10 GHz, with the diameter being larger at lower frequencies and smaller at higher frequencies within the band. With the finite illumination area and because these compact probes are easily integrated into an automated positioning system, they are termed “advanced microwave mapping probes” (AMMP).

3. Example Measurements

In a factory setting, direct measurements of manufactured components or parts are often used for quality assurance (QA) and feedback purposes so that manufacturing defects are identified early in the process and manufacturing processes are corrected. Furthermore, in the manufacture of large or expensive parts, QA requirements may necessitate measurement of every part that is produced. A compact spot probe such as the AMMP described above enables this by ease of integration into factory automation systems. This paper presents some measurement examples that utilize these microwave mapping probes integrated onto industrial robots, thus demonstrating their usefulness for manufacturing QA.

3.1 Multilayer Dielectric/Conductive Composites

The first QA example shows the use of a spot probe to map the electromagnetic properties of a multi-layer material: a dielectric window with a conductive coating for electromagnetic interference (EMI) mitigation. In other words, the conductive coating is designed to minimize transmission of microwave energy while still enabling optical transmission. The photograph on the left side of Figure 2 shows a microwave mapping probe mounted on an industrial robot. The probe is aimed at a material specimen consisting of an acrylic substrate that is coated with a conductive layer of commercial window tint. The acrylic layer was approximately 25 mm thick. The window tint is conductive with a nominal sheet impedance of approximately 10 ohms per square. On the lower left quadrant of the test specimen, an additional layer of 12.7 mm thick acrylic was added, and on the upper right quadrant of the specimen, an additional layer of 50 ohm per square window tint was added. The robot path was programmed to raster scan the part with measurements made at a grid of locations every 2 cm. Not shown is a second robot and microwave mapping probe that is placed on the other side of the test part. The robots operated in a coordinated fashion so that the probes were aligned along a common axis and transmission loss through the part was measured.

A microwave network analyzer was used to collect data from 2 to 18 GHz by stepping through 1601 different frequency measurements. A simple ‘response’ calibration of the data was done with a measurement of a ‘clear-site,’ which consists of a single measurement of nothing (empty space) in between the microwave mapping probes. The calibrated insertion loss is calculated as a ratio of the insertion loss with the specimen to the insertion loss of the clear-site. For both the calibration and the part measurement, the probes were separated by a distance of 14 cm (5.5”). Additionally, the data were processed with time-domain methods to eliminate errors caused by multipath reflections. In particular, the frequency data were transformed into time domain via Fourier transform methods. The desired signal corresponding to the part under test was identified, and spurious signals outside of the desired signal were eliminated before transforming the measured data back into frequency domain. For the data shown in this paper, a 0.5 nanosecond window width was used for this purpose.

Once processed, the insertion loss data can then be used to invert the desired properties of the material under test. In this case the substrate thickness and the sheet impedance of the

conductive layer were calculated. Using standard cascade matrix methods or transmission line theory, an expression relating the transmission (S_{21}) to the thickness (d) and sheet impedance (Z_s) of this two-layer material can be derived [1],

$$S_{21} = \frac{2Z_s(\Gamma^2-1)\mathrm{T}}{(2Z_s+Z_0)(\Gamma^2\mathrm{T}^2-1)+Z_0(\mathrm{T}^2-1)}, \quad (1)$$

where Z_0 is the impedance of free space, $\Gamma = (\mu - \sqrt{\mu\varepsilon})/(\mu + \sqrt{\mu\varepsilon})$ and $T = e^{-ik_0 d\sqrt{\mu\varepsilon}}$. Additionally, ε and μ are the relative permittivity and permeability, and k_0 is the wave number in free space.

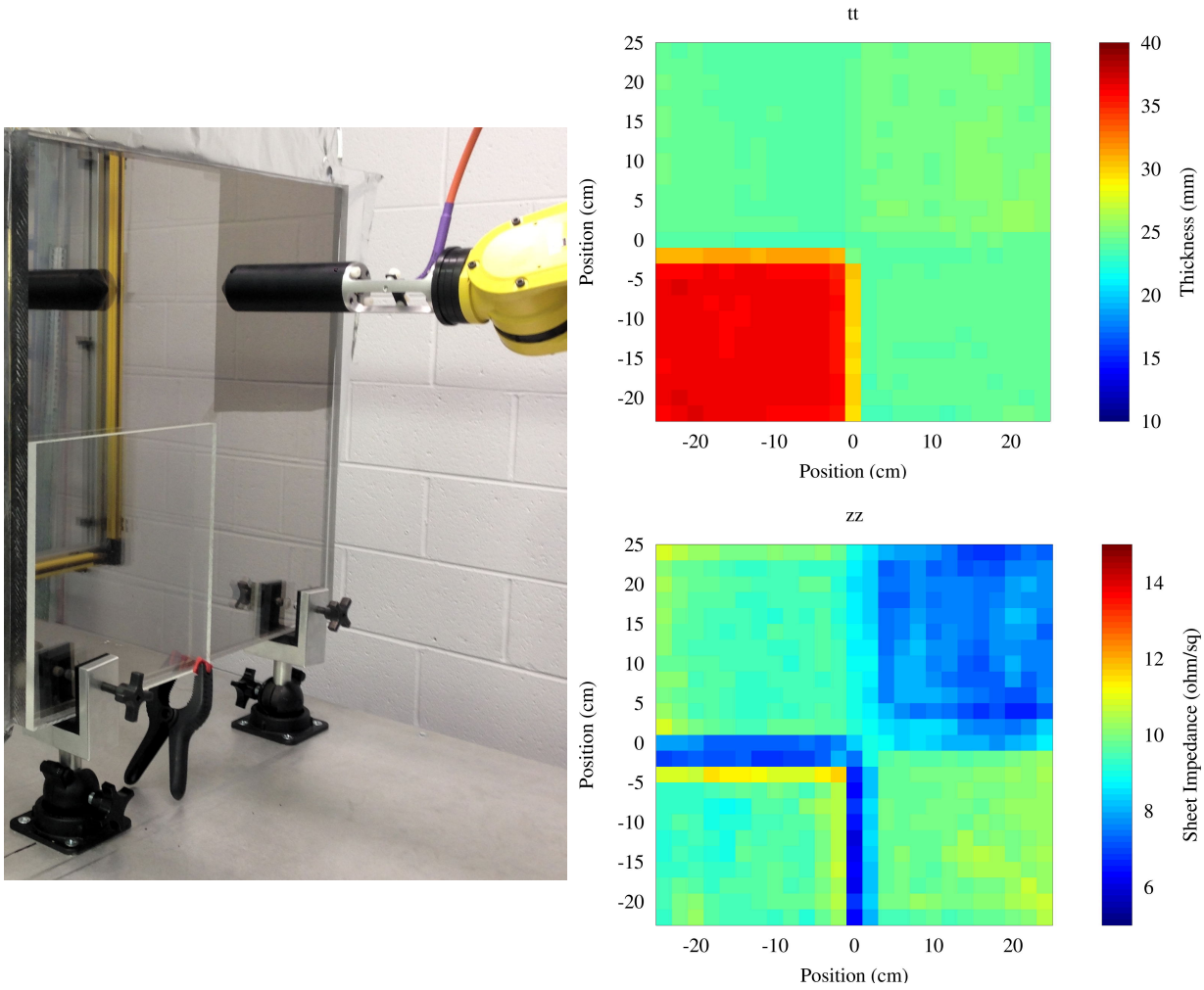

Figure 2. (left) Photograph of microwave mapping probe on a robotic arm scanning a material specimen consisting of an acrylic substrate coated with conductive window tint. (right, top) A positional map of the inverted substrate thickness. (right, bottom) A positional map of the inverted sheet impedance of the coating.

Since the substrate was acrylic, its relative permittivity (ε = 2.6) was already known and was assumed fixed in the inversion calculation. The inverted substrate thickness and sheet impedance shown on the right side of Figure 2 were obtained by minimizing the difference between Equation (1) and the measured S_{21} data using a standard multivariate minimization algorithm [5]. As the data on the right side of Figure 2 show, the microwave mapping probe measurements combined with the data processing described above are able to accurately

identify the substrate thickness and the sheet impedance of the conductive coating as a function of position.

In the upper-right thickness plot, the bottom-left quadrant of the specimen has an additional acrylic layer added. The plotted data accurately show the combined thickness of both 25 mm and 12.7 mm layers in this quadrant. In the bottom-right sheet impedance plot, most of the measured data show the approximately 10 ohm/square sheet impedance of the base window tint layer, while the upper right quadrant of the specimen shows a measured sheet impedance closer to 8 ohm/square, corresponding to the 50 ohm and 10 ohm window tints in parallel. Note that the algorithm misidentifies the sheet impedance at the border between the thicker acrylic and the thinner acrylic. This is because there is a 12.7 mm step in the acrylic thickness, which scatters microwave energy to other angles besides normal incidence, causing an apparent reduction in the locally transmitted microwave energy.

3.2 Delamination in Glass Reinforced Composites

Another potential application for these microwave mapping probes is in the detection of defects in structural composites. One common type of defect that is of concern for structural rigidity is the delamination or separation between laminate layers. Delamination can occur as a result of weak adhesive bonding between the fibers and the matrix. Figure 3 shows a calculation of the effect of delamination on the microwave properties of a dielectric composite with a relative permittivity of $4.5 - 0.1i$. These data were calculated with one-dimensional transmission line theory.

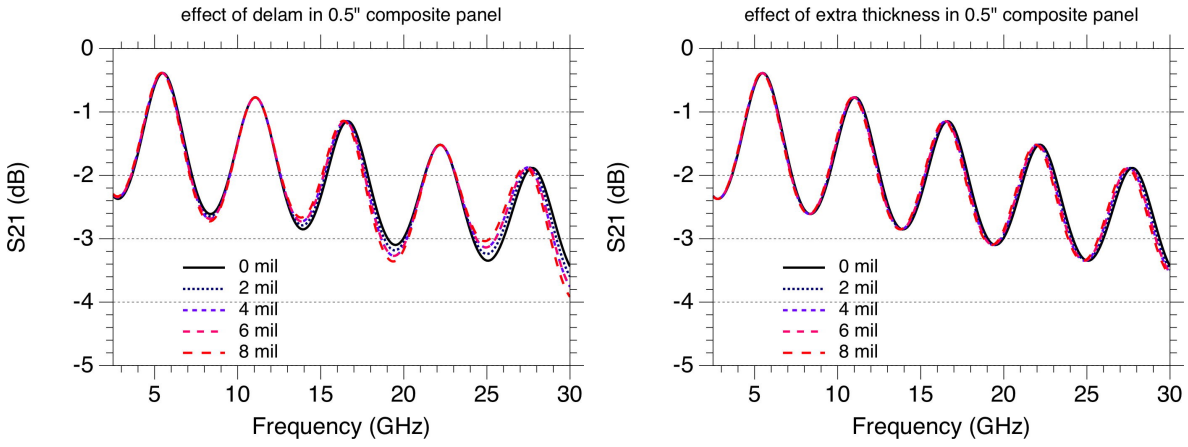

Figure 3. Calculated transmission amplitude (S_{21}) for a 12.7 mm (0.5") thick fiberglass panel with a delamination gap in the middle (left) and with a small increase in thickness (right). 1 mil = 0.0254 mm.

The plot on the left side of Figure 3 shows the transmission coefficient (S_{21}) that would occur in a 12.7 mm (0.5") fiberglass composite with a small air gap layer in the middle. The different curves in this plot correspond to various gap widths up to 0.2 mm (8 mil). The data show a small but detectable perturbation of the transmission coefficient compared to a solid composite with no delamination gap. Note that the periodic characteristic of these curves is due to constructive and destructive interference between the front and rear faces of the composite panel; and the periodicity is driven by the overall thickness of the fiberglass slab relative to microwave wavelength. While this calculation shows the ideal case where the thickness of the slab is well known, an important question is: Can we distinguish between the effects of a delamination gap versus a variation in the overall thickness of the composite

when thickness is not well known or consistent? To answer this, the right side of Figure 3 shows the effect on the transmission coefficient as the overall thickness is varied in a composite with no delamination. In this case, the transmission coefficient is also perturbed, but close examination of the data show that the character of that perturbation is different than it is with the delamination gap.

A clearer picture of the difference caused by a delamination gap versus simple thickness variation can be seen in Figure 4. The curves in Figure 4 are simply the same data of Figure 3, but replotted after first dividing them by the S_{21} of the ideal or reference 12.7 mm composite. As in Figure 3, the left side of Figure 4 shows the effect of varying the delamination gap, while the right side of Figure 4 shows the effect of varying the overall thickness on a non-delaminated composite. Without a delamination, the change in thickness imposes a simple oscillation with a monotonically growing envelope. In contrast, the effect of a delamination gap in the middle of the slab is to impose a much more complicated growing oscillation. This subtle behavior makes it difficult to identify a simple parameter with which to gauge the presence and severity of a delamination gap.

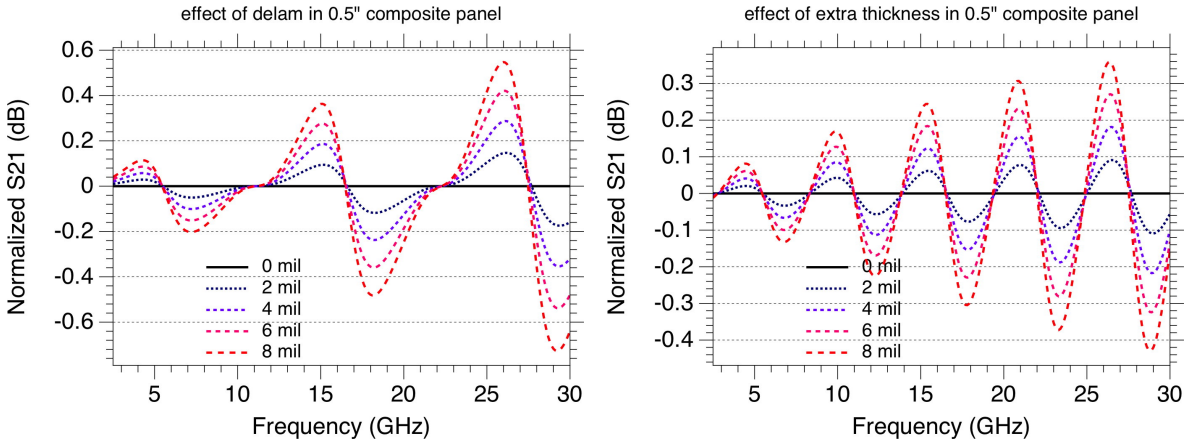

Figure 4. Calculated transmission amplitude normalized to an ideal 12.7 mm thick panel for a 12.7 mm (0.5") thick fiberglass panel with a delamination gap in the middle (left) and with a small increase in thickness (right). 1 mil = 0.0254 mm.

In a similar vein, Figure 5 shows the effect of delamination (left plot) versus overall thickness variation (right plot) on the reflection coefficient (S_{11}), after it has been normalized by the reflection from the ideal composite panel. Thus in either reflection or transmission, these theoretical results show that there is a subtle difference in the microwave behavior of an internal gap versus thickness variations. A key feature, however, is that the detection of these behaviors requires measurement over a sufficiently broad frequency range to capture the oscillatory nature of the effect.

To validate these theoretical results, an experiment was conducted using the microwave mapping probes described above. Figure 6 includes a photograph of the experiment, in which the probes were mounted on industrial robots. The probes were moved in a vertical line and measured the reflection and transmission coefficient every 2 cm along that vertical scan. The composite panel pictured in the photograph is actually two separate 6.35 mm thick panels placed adjacent to each other. The bottom of the panels were clamped tightly to minimize the air gap between them. At the top of the panels, small plastic spacers were inserted between the two panels to create an air gap that simulates delamination. The spacers were just under

0.5 mm (18 mils) thick so the gap varied from negligibly small at the bottom to a maximum of 0.5 mm along the direction of the robot scan.

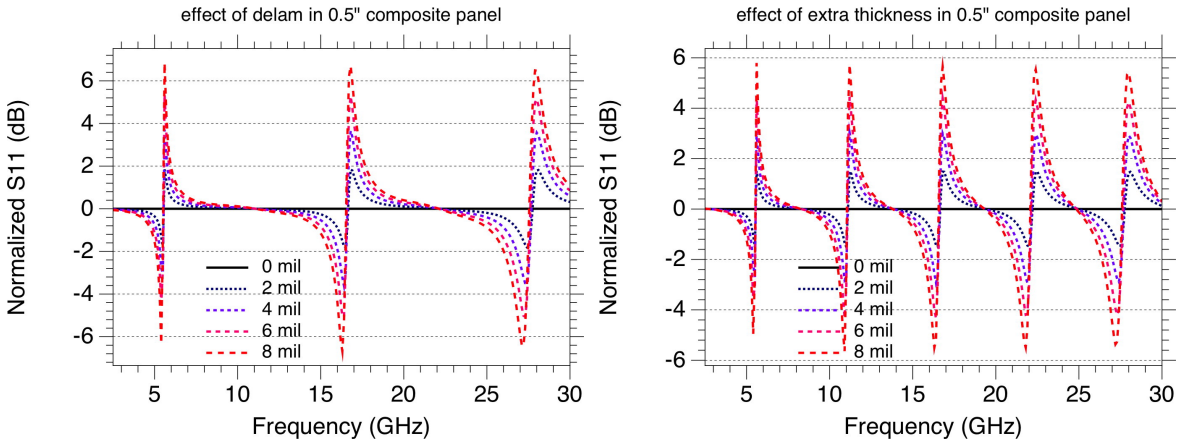

Figure 5. Calculated reflection amplitude normalized to an ideal 12.7 mm thick panel for a 12.7 mm (0.5") thick fiberglass panel with a delamination gap in the middle (left) and with a small increase in thickness (right). 1 mil = 0.0254 mm.

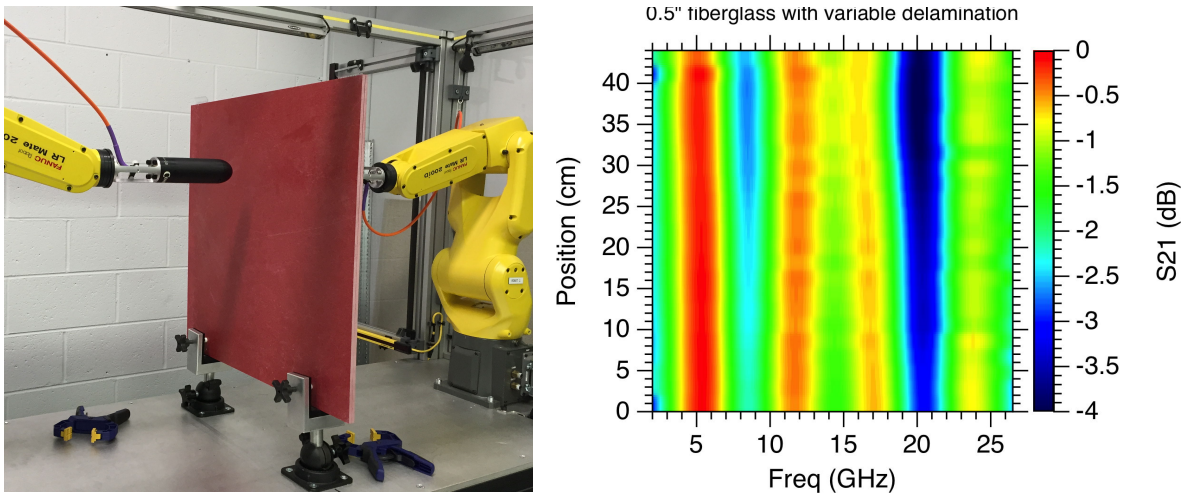

Figure 6. (left) Photograph of robotic scan system measuring fiberglass panels. (right) Measured transmission amplitude (S21) for two adjacent 6.35 mm thick fiberglass panels with a variable delamination gap in between.

Shown on the right side of Figure 6 is a plot of the collected transmission (S_{21}) data as a function of frequency and position. A position of 0 cm corresponds to near the bottom while 44 cm corresponds to a position near the top of the fiberglass specimen. Consistent with the theoretical calculations shown previously, there is a small change in the spectral characteristics of the microwave transmission as the air gap in the middle of the material widens.

As the theoretical results earlier showed, it is possible to distinguish between a delamination gap and a simple thickness change by looking at the spectral characteristics of the microwave transmission or reflection. However the data analysis is necessarily complicated since there is not a single feature of the spectrum that can be attributed to a gap, but that would be otherwise independent of any thickness variation. To overcome this problem, a more sophisticated analysis was conducted on the measured transmission and reflection data to

attempt to separate out thickness effects from delamination. This analysis consisted of fitting the measured data to an analytical model of an ideal composite slab with no delamination. Specifically a multivariate fit of thickness and dielectric permittivity were made to all the measured data, whether or not there was a delamination gap. The reason for including permittivity as a variable fit parameter is that in many situations the dielectric permittivity may not be exactly known.

Without a delamination, the data should fit the ideal theoretical model with minimal error. When a delamination is present, then the fit will not be exact and there will be a small but finite difference between the measured microwave parameters and the theoretical model. The idea is that this finite difference is related primarily to the presence of the delamination gap. Summing this residual error over the measured frequencies should then give an indication of the size of an air gap associated with the delamination,

$$S_{xx}^{residual} = \sqrt{\Sigma_{frequency}\left(\left|S_{xx}^{theory}\right| - \left|S_{xx}^{measured}\right|\right)^2} \qquad (2)$$

Note that this equation only uses the amplitude and does not require the phase of the measured S-parameters. This can be advantageous for measurements in a factory or field environment since it reduces the importance of exact positioning of the microwave mapping probes.

This processing was applied to the measured data for the specimen pictured in Figure 6. A multivariate fit algorithm similar to the multilayer example discussed above was used. The S-parameters from each measurement location were fit to obtain a best thickness and permittivity, and the summed residual fit-error as a function of probe position is plotted in Figure 7. The left side of Figure 7 shows the residual for transmission (S_{21}) data while the right side plots the residual for reflection (S_{11}) data. Both figures have two curves: (a) one corresponding to the fiberglass panels with a continuously varying gap between them and (b) one corresponding to the fiberglass panels tightly clamped both on the top and bottom. The residual for the fully clamped specimen is unchanging with position, indicating that there is no significant gap between them. The residual for the specimen with an air gap in the middle is monotonically increasing, corresponding to the varying gap width going from the clamped bottom of the fiberglass to the top, which has a ~0.5 mm spacer inserted.

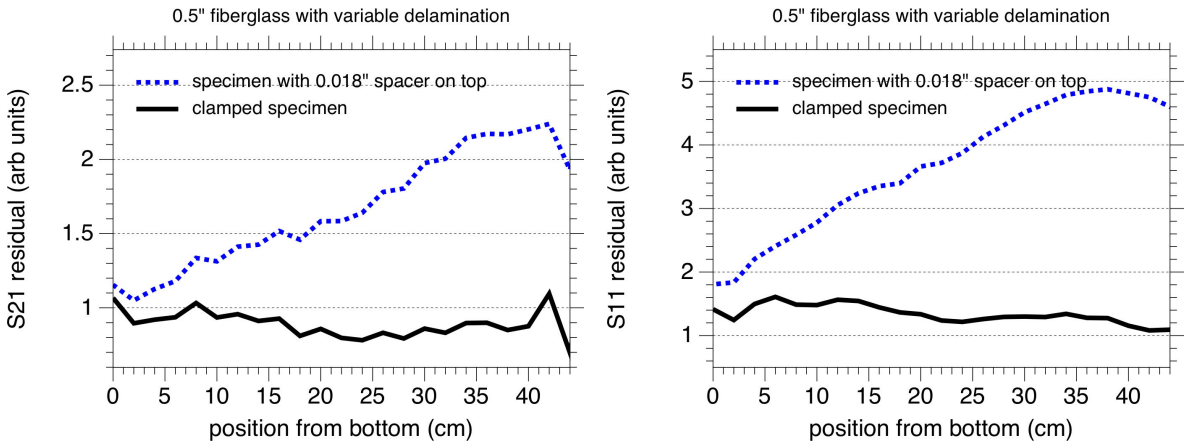

Figure 7. Calculated residual S21 (left) and S11 (right) for the two fiberglass panels with and without the delamination gap. This residual signal is proportional to the width of the delamination gap.

Ideally the fully clamped specimen should have a residual signal of 0. Instead Figure 7 shows that there is a nonzero baseline residual error. This may be in part because the fit algorithm assumes that the permittivity is single-valued and not a function of frequency. In reality the permittivity may vary slightly with frequency. Additional error sources may include measurement uncertainty, material inhomogeneity (i.e. if voids are present, variations in the fiber weave, etc.), and the fact that even when clamped, surface roughness of the fiberglass induces a very small air gap layer. Also of note is the fact that the residual signal is both stronger and less noisy for reflection than for transmission (even though the transmission and reflection residuals were summed over the same number of frequency points).

4. Conclusions

A new wideband probe technology was presented, which draws inspiration from dielectric rod antennas. By optimizing both the metallic and dielectric elements of this probe, it is more compact and has wider frequency bandwidth than previous microwave sensor technologies. Application of this microwave-mapping probe on two NDE quality assurance examples is shown. First, a pair of probes is demonstrated as a way to accurately measure multilayer electromagnetic materials in-situ. Utilizing the measured insertion loss combined with some a-priori knowledge about the material enables inversion of intrinsic properties such as layer thickness and conductive sheet impedance. In the second example the probes are shown to have the ability to detect small internal delamination gaps in a fiber reinforced polymer composite. An iterative fit algorithm is used to separate the effects of a delamination from overall thickness variations. The algorithm relies only on the measured amplitude and can be applied either to transmission or reflection measurements. Both of these examples rely on wide bandwidth data to provide sufficient information for ascertaining the desired intrinsic properties.

References

1. J Schultz, Focused Beam Methods, ISBN 1480092851, 2012
2. J Musil, F Zacek, A Burger, J Karlovsky, “New Microwave System to Determine the Complex Permittivity of Small Dielectric and Semiconducting Samples,” 4th European Microwave Conference, 66-70, 1974
3. R Diaz, J Peebles, R Lebaron, Z Zhang, L Lozano-Plata, “Compact Broad-Band Admittance Tunnel Incorporating Gaussian Beam Antennas,” U.S Patent 7889148, 2007
4. J Schultz, J Maloney, K Cummings-Maloney, R Schultz, J Calzada, B Foos, “A Comparison of Material Measurement Accuracy of RF Spot Probes to a Lens-Based Focused Beam System,” Proceedings of the 2014 AMTA, Tucson AZ, 2014
5. W Press, S Teukolsky, W Vetterling, B Flannery, Numerical Recipes in C, the Art of Scientific Computing, 2nd ed. Cambridge University Press, 1992